

## Removal of Phenol and 4-Chlorophenol from Aqueous Solutions by Olive Stone-based Activated Carbon

Mourad Termoul<sup>1</sup>, Benaouda Bestani<sup>1</sup>, Nouredine Benderdouche<sup>1\*</sup>, Mostefa Belhakem<sup>1</sup> and Emmanuel Naffrechoux<sup>2</sup> (1) *Département de Chimie, Faculté des Sciences et Sciences de l'Ingénieur, B.P. 188, Mostaganem 27000, Algeria.* (2) *Laboratoire ESIGEC, Université de Savoie, Chambéry, France.*

(Received 10 July 2006; accepted 25 September 2006)

**ABSTRACT:** The evaluation of agricultural by-products as a means of removing pollutants from contaminated wastewater is attracting increasing interest for sustainable development applications. The present work deals with the removal of phenol and 4-chlorophenol from aqueous solutions by chemically activated olive stones. The olive stones were soaked in 50% phosphoric acid for 3 h at 443 K. After washing, the product was activated in an inert atmosphere for 2 h or 3 h at temperatures within the range 873–1023 K. The carbons thus prepared were characterized by Methylene Blue and iodine adsorption, N<sub>2</sub> adsorption at 77 K in conjunction with the BET equation, scanning electron microscopy (SEM) and Boehm titrations. The sorption capacity towards both pollutants was determined by fitting the Langmuir model to the adsorption isotherms. The optimum activation temperature and time were 1023 K and 3 h, respectively. A maximum adsorption capacity of 189 mg/g was obtained for phenol and 436 mg/g for 4-chlorophenol. In comparison, the Merck and Aldrich commercial-grade powdered activated carbons ranked lower with adsorption capacities of 145 mg/g and 179 mg/g for phenol and 244 mg/g and 316 mg/g for 4-chlorophenol, respectively.

## INTRODUCTION

Chlorophenols are toxic members of a class of compounds of chlorinated and nitro-substituted phenols used as pesticides and anti-bacterials. 4-Chlorophenol is used as an intermediate in the preparation of higher chlorinated phenols. Contamination of the environment by 4-chlorophenol and phenol can be attributed to a number of industrial processes, including chemical, petrochemical and agricultural. Due to their high toxicity, they are often classified as priority pollutants by environmental agencies worldwide (Gimeno *et al.* 2005; Alavarez *et al.* 2005). Most often, treatment methods are not cost-effective and sometimes not suitable (Milner and Goulder 1986).

Activated carbon is widely used for the removal of pollutants from gaseous and liquid phases. However, rising production costs somewhat hinder its general development. As a result, natural wastes and plants have drawn growing attention during the last few years for pollution control applications (Yan and Viraraghavan 2000; Gardea-Torresdey *et al.* 1998; Plaza de los Reyes *et al.* 1997; Ng *et al.* 2003; Benderdouche *et al.* 2003). Some agricultural by-products, such as those derived from olive industries and fruit stones, have also been used as precursors for the

\*Author to whom all correspondence should be addressed. E-mail: benderdouchen@yahoo.fr.

preparation of activated carbon (Galiatsatou *et al.* 2001; Martinez *et al.* 2003; Aygün *et al.* 2003). In Algeria, most of the olive waste produced is incinerated or disposed of into the environment. However, through the development of the arboreal agro-industry in the near future, the generation of huge amounts of such wastes could cause further pressure on the environment and disposal costs.

Chemical activation reduces the formation of tar and other by-products, thereby increasing carbon yield (Gonzales-Serrano *et al.* 1997). Several chemical agents such as phosphoric acid, zinc chloride, potassium hydroxide (Molina-Sabio and Rodriguez-Reinoso 2004) have been used to prepare activated carbons chemically. Due to environmental risks, phosphoric acid has become a widely accepted chemical activator (Gómez-Serrano *et al.* 2005). The preparation of activated carbon is influenced by many factors, which include activation time and temperature. In the present work, we prepared a series of activated carbons by varying the activation temperature from 873 K to 1023 K at activation times of 2 h and 3 h.

Characterization of the activated carbons has mainly focused on the determination of surface area. Additional information was obtained by comparing the adsorption characteristics towards Methylene Blue and iodine. Methylene Blue adsorption is often used to characterize the mesoporosity of activated carbons, as well as providing a model for the adsorption of visible organic pollutants from aqueous solutions (Lucier *et al.* 1994). The iodine number is an important parameter for characterizing the surface area of microporous carbons, particularly those with small molecules (Noszko *et al.* 1984). Scanning electron microscopy was used to monitor the development of texture and porosity in the prepared active carbons. Surface functional groups were characterized by the Boehm method, since they are also important in determining the adsorption capacity in conjunction with the total surface area (Boehm 1994).

## MATERIALS AND METHODS

### Materials

The olive stones were collected from an olive plant discharge in the Sig area (west of Algeria), washed, dried overnight at 383 K and crushed in a Vierzen grinder. The particles were then soaked in 50% phosphoric acid solution for 3 h at 443 K. The residue was washed in 0.1 N hydrochloric acid solution, followed by repeated washing with laboratory-produced hot distilled water until the filtrate was free from phosphate ions as shown by conductivity measurements and lead acetate tests. Activation was carried out under a nitrogen atmosphere in a tubular furnace at 873, 923, 973 and 1023 K for 2- and 3-h activation times. The prepared activated carbons were dried at 383 K for 24 h, and then ground and sieved to obtain a particle size of < 71  $\mu\text{m}$ . The adsorptive performance of these products was compared with that of two well-known commercial-grade activated carbons obtained from Merck and Aldrich.

### Methods

#### *Surface characterization*

Nitrogen adsorption at 77 K was used to determine the specific surface areas. A manometric gas adsorption Sorptomatic apparatus was used in the nitrogen adsorption experiments. Samples (0.04 g) were degassed at 573 K for 4 h. Their specific surface areas were determined via

the BET equation, while their micropore volumes and mean pore radii were determined using the Dubinin–Stoeckli fit. The nitrogen surface areas were obtained using a value of  $0.162 \text{ nm}^2$  for the molecular area of  $\text{N}_2$  at 77 K. A mean saturation pressure of 778.4 mmHg was applied.

Methylene Blue adsorption and iodine number were respectively utilized to monitor the development of the meso- and micro-porosities of the prepared activated carbons.

The functional groups present on the surface of the activated carbon may include carboxyls, phenols, lactones and/or quinones (Leon y Leon and Radovic 1992; Mattson and Mark 1971). Carboxylic groups and lactones are acidic in nature and produce negatively charged sites on the carbon surface. Phenolic hydroxyls confer some acidity to the carbon surface whereas quinones are neutral with some hydrophobic character (Goyal *et al.* 2001; Bansal *et al.* 1977). The method proposed by Boehm (1966) was used to determine the acidity of the activated carbon surface.

### Adsorption tests

Phenol and 4-chlorophenol were employed as the liquid-phase pollutants in the adsorption experiments. The adsorption isotherms of these compounds onto the activated carbon samples were obtained by adding 0.1 g of a given activated carbon to several flasks containing 25 ml of aqueous solutions with different initial known concentrations of either phenol or 4-chlorophenol. These flasks were agitated for 2 h at ambient temperature (this equilibrium time having been determined by kinetic tests). The suspensions were then filtered and the equilibrium concentrations determined spectrophotometrically at the maximum UV absorption wavelength of 270 nm for phenol and 281 nm for 4-chlorophenol, with a visible wavelength of 660 nm being employed for Methylene Blue. Iodine concentrations were determined volumetrically using 0.1 N sodium thiosulphate with thyodene as an indicator. The adsorption capacities of the carbon samples towards Methylene Blue, phenol and 4-chlorophenol were calculated by applying the Langmuir equation.

## RESULTS AND DISCUSSION

### Weight loss versus activation temperature and time

Figure 1 shows plots of the percentage weight loss and burn-off as a function of the activation temperature for the olive stone materials. It will be seen from the figure that most of the weight loss occurred during carbonization where rudimentary pores formed and volatile organic matter disappeared. An increased development of porosity occurred during burn-off. Increasing activation time and temperature enhanced this development leading to the creation of more and more pores (El-Sheikh *et al.* 2004). Thus, activation for 3 h at a temperature of 1023 K resulted in 81% weight loss and 86% burn-off, yielding increased porosity. These end-conditions were chosen for subsequent experiments to avoid further mass loss and to preserve the low-cost quality of the prepared material.

### Iodine and Methylene Blue adsorption

ASTM standard D4607 was employed to determine the iodine number (ASTM 1999). An important physicochemical quantity for evaluating an adsorption process is the equilibrium

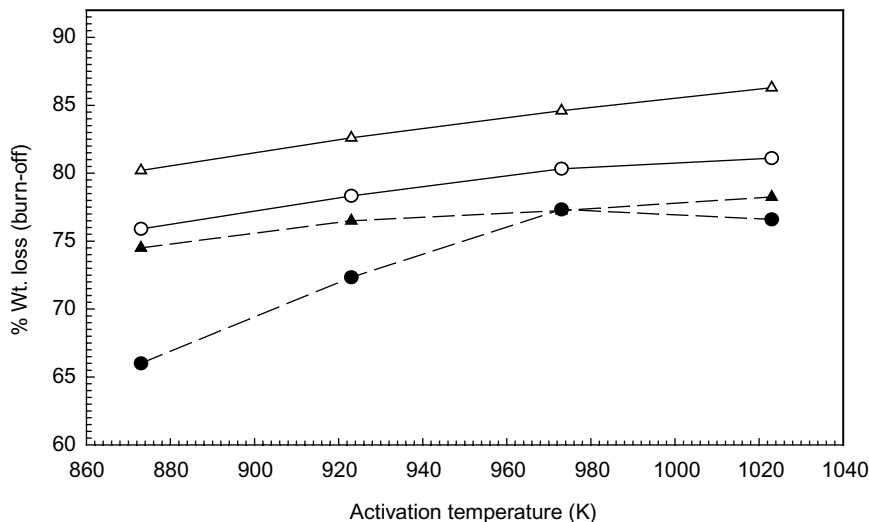


**Figure 1.** Influence of activation temperature and time on the percentage weight loss and burn-off of the olive stone samples studied. Data points relate to the variation in weight loss (circles) and burn-off (triangles) after the following activation times: ●, 2 h; ○, 3 h; ▲, 2 h; △, 3 h.

adsorption which gives the capacity of the adsorbent. To calculate this quantity, the adsorption equilibrium isotherms for Methylene Blue, phenol and 4-chlorophenol onto the various activated carbons were fitted with the Langmuir equation:

$$\frac{x}{m} = \frac{KbC_{eq}}{1 + KC_{eq}} \quad (1)$$

where  $x/m$  (mg/g) is the adsorption density,  $K$  (l/mg) is a constant related to the adsorption energy (Benderdouche *et al.* 2003; Hamadi *et al.* 2001),  $b$  (mg/g) is the maximum adsorption capacity corresponding to complete monolayer coverage and  $C_{eq}$  (mg/l) is the equilibrium concentration of the solute. The results of the iodine number and Methylene Blue uptake measurements after various times and at different activation temperatures are summarized in Figure 2.

The iodine number steadily increased with activation time and temperature until it reached a value of 1012 mg/g for activation for 3 h at 1023 K, indicating that this procedure led to the development of a highly porous structure. Similarly, the adsorption capacity for Methylene Blue also increased up to 485 mg/g with activation time and temperature due to pore opening and enlargement, resulting in the development of increased mesoporosity during the activation process. Since Methylene Blue dye is cationic in aqueous solution, the increased uptake may also be explained in terms of solute-carbon surface interactions. In comparison, the results for the commercial-grade Merck and Aldrich activated carbons were 828 mg/g and 883 mg/g, respectively, for iodine number uptake and 357 mg/g and 417 mg/g, respectively, for Methylene Blue uptake. In comparison, some adsorption capacities investigated for Methylene Blue onto olive seed wastes cited in the literature attained values of 300 m<sup>2</sup>/g (El-Sheikh *et al.* 2004) and 263 m<sup>2</sup>/g (Stavropoulos and Zabaniotou 2005). As a consequence of the above data, all subsequent activated carbon preparations were performed at 1023 K for 3 h.

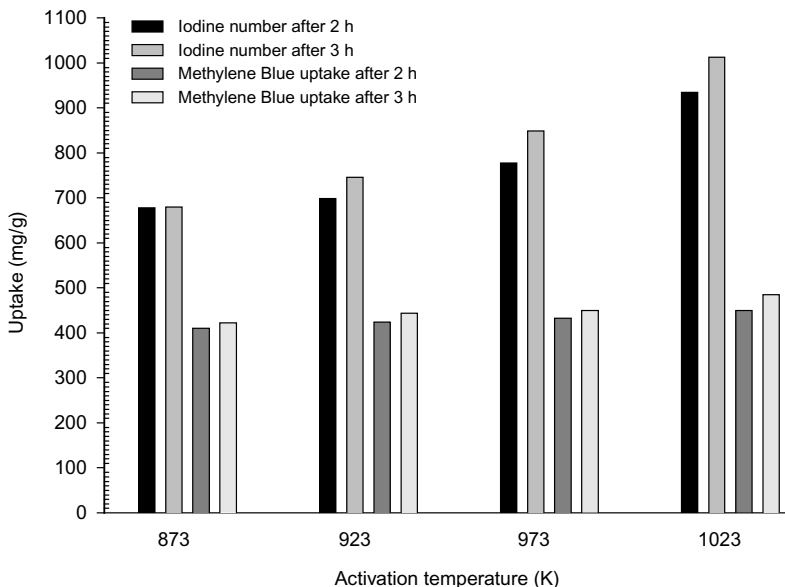


**Figure 2.** Influence of activation temperature and time on the iodine number and Methylene Blue uptake of the olive stone activated carbons prepared.

### Determination of surface functional groups

Table 1 summarizes the results for the surface functional groups on the various carbons investigated as determined by the Boehm method. The olive-stone activated carbon showed a higher acidic content than its commercial-grade counterparts, since the total capacity of oxide groups was increased by phosphoric acid activation.

### Gas adsorption test

Figure 3 depicts the BET isotherms obtained for the Merck, Aldrich and olive-stone activated carbons (AC). The adsorption isotherm for the Merck activated carbon was type I in the BDDT classification, presenting a sharp increase in nitrogen uptake at relatively small pressures, a plateau for intermediate pressures and finally a gradual and small increase at high pressures. The olive stone- and Aldrich-activated carbons exhibited more complex adsorption isotherms characterized by a continuous increase in nitrogen uptake even at high pressures, corresponding to multilayer coverage of mixed microporous/mesoporous materials.

**TABLE 1.** Concentration of Functional Groups (mequiv/g) on the Activated Carbon (AC) Surfaces

Adsorbent	Carboxylic acids	Lactones	Phenols
Olive-stone AC	1.33	1.25	0.31
Merck AC	0.56	1.14	0.93
Aldrich AC	0.12	1.17	1.16

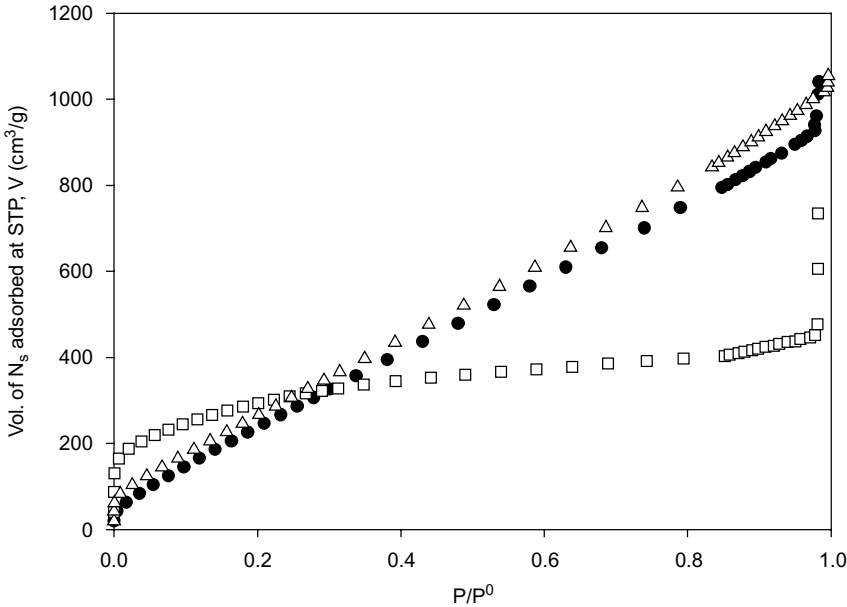


**Figure 3.** BET adsorption isotherms for the activated carbon (AC) samples studied. The data points correspond to the following samples: ●, olive stone AC; □, Merck AC; △, Aldrich AC.

The Dubinin–Stoeckli (DS) equation incorporates a Gaussian distribution of pore half-widths in its description of the adsorption of gases and vapours onto heterogeneous microporous adsorbents (Dubinin 1989). If it is assumed that the micropore-size distribution in the adsorbents studied was Gaussian in nature, the following equation can be used to describe the adsorption of gases and vapours onto heterogeneous microporous adsorbents with slit-shaped pores, where  $x$  is the normal half-width distribution of micropore volumes ( $W_0$ ) for the slit-pore model. The normal distribution equation is given by:

$$\frac{d(W_0)}{d(x)} = \frac{W_0^0}{\partial\sqrt{2\pi}} \exp\left(-\frac{(x_0 - x)^2}{2\partial^2}\right) \tag{2}$$

where  $W_0^0$  corresponds to the total volume of supermicropores and micropores,  $x_0$  is the modal micropore half-width for the distribution and  $\partial$  is the variance of the pore half-width. For adsorbents with a heterogeneous micropore structure, the Dubinin–Stoeckli adsorption equation may be written as:

$$W = \frac{W_0^0}{2\sqrt{1 + 2m\partial^2A^2}} \exp\left[-\frac{mx_0^2A^2}{\sqrt{1 + 2m\partial^2A^2}}\right] \left[1 + \operatorname{erf}\left(\frac{x_0}{\partial\sqrt{2}\sqrt{1 + 2m\partial^2A^2}}\right)\right] \tag{3}$$

where  $A$  is the maximum differential molar work ( $A = -\Delta G$ , the Gibbs free energy) needed to transport 1 mol of adsorbate from the liquid or gaseous phase to the surface of an infinitely large amount of adsorbent,  $m = (1/\beta k)^2$  where  $\beta$  is the affinity coefficient specific to a given adsorbate and  $k$  is the characteristic energy constant introduced by Dubinin (1985).

This method has been used to fit the present adsorption data over the pressure range corresponding to the DS equation ( $0.0 < P/P^0 < 0.5$ ) using values of 13 kJ/(nm mol) and 0.33 for  $k$  and  $\beta$ , respectively. Figure 4 depicts the extent of the pore-size distributions for the activated carbons studied, which varied with increasing surface area. The modal size distribution was centred similarly for the olive stone and Aldrich adsorbents but differently for the Merck material. On the other hand, the Merck sample exhibited a narrower pore-size distribution and a smaller mean pore radius. The high surface area obtained for the prepared activated carbon accorded with its high iodine number value and Methylene Blue adsorption capacity.

The BET surface areas ( $\text{m}^2/\text{g}$ ) were computed from the linear portions of the BET lines (not shown) over the  $0.1-0.3P/P^0$  range. The Dubinin–Stoeckli (DS) fit applied to the various data allowed the micropore volumes and the mean pore radii to be determined. The results are reported in Table 2, which also includes the surface occupied by Methylene Blue,  $S_{\text{MB}}$ , as determined from the Methylene Blue monolayer coverage adsorption capacity calculations, taking  $1.19 \text{ nm}^2$  as the molecular area (Goyal *et al.* 2004).

The surface area,  $S_{\text{BET}}$  ( $\text{m}^2/\text{g}$ ), obtained for the activated carbon prepared from olive stones was higher than that of the Merck commercial-grade adsorbent, approaching that of the Aldrich activated carbon which was the highest. The magnitude of  $S_{\text{BET}}$  should be greater than the Methylene Blue monolayer capacity-based surface area due to the difference in the molecular size of nitrogen and Methylene Blue molecules. The ratio  $S_{\text{MB}}/S_{\text{BET}}$  indicates the proportion of surface area available for the larger Methylene Blue molecule. This ratio was greatest for the olive stone activated carbon suggesting that the porosity was associated with a more heterogeneous or mixed micropore/mesopore structure. However, the presence of carbon–oxygen groups also had an influence on the adsorbate uptake by providing sites for supplementary adsorption. This may be the reason for the high adsorption capacity.

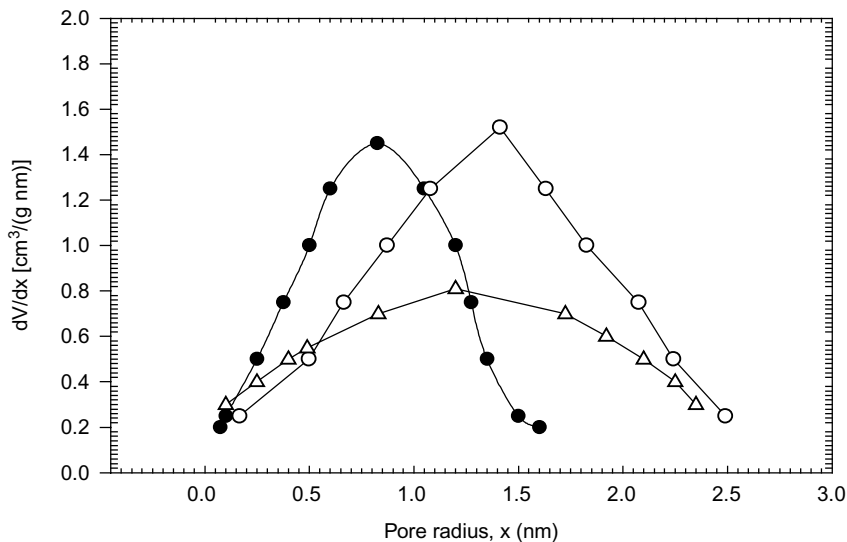


**Figure 4.** Pore-size distributions for the activated carbon (AC) samples studied as obtained via the Dubinin–Stoeckli method and using  $\text{N}_2$  as an adsorbate at 77 K. Data points correspond to the following samples: ●, Merck AC, ○, olive stone AC; △, Aldrich AC.

**TABLE 2.** BET Surface Areas,  $S_{\text{BET}}$ , Methylene Blue-occupied Surface Areas,  $S_{\text{MB}}$ , Micropore Volumes and Mean Pore Radii of the Activated Carbons (AC) Studied

Sample	$S_{\text{BET}}$ ( $\text{m}^2/\text{g}$ )	$S_{\text{MB}}$ ( $\text{m}^2/\text{g}$ )	$S_{\text{MB}}/S_{\text{BET}}$	Micropore volume ( $\text{cm}^3/\text{g}$ )	Mean pore radius (nm)
Olive-stone AC	1257	1087	0.86	0.29	1.55
Merck AC	1031	800	0.78	0.43	0.83
Aldrich AC	1301	934	0.72	0.48	1.20

### SEM characterization

The scanning electron micrographs of the three activated carbons (olive stone, Merck and Aldrich) prepared by heating for 3 h at 1023 K are shown in Figure 5. At a magnification of 200 $\times$ , the micrographs show that the prepared olive stone samples exhibited a uniform structure. Such

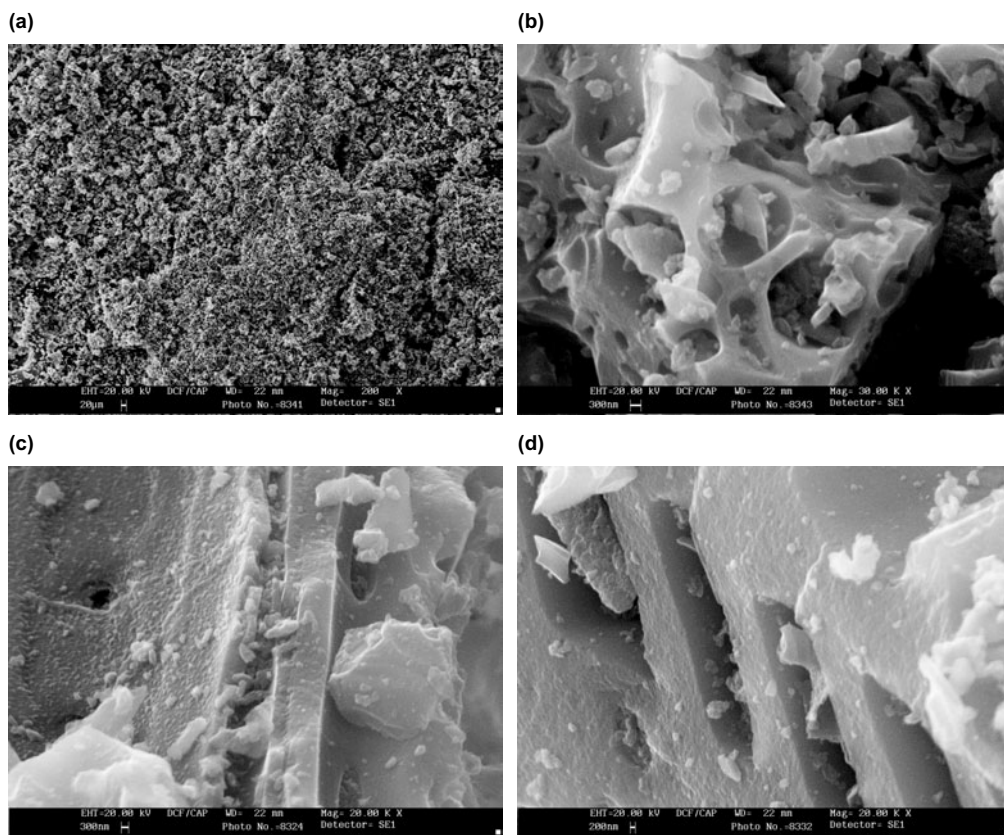


**Figure 5.** SEM micrographs of the activated carbon (AC) samples studied: (a) olive stone AC, magnification 200 $\times$  ; (b) olive stone AC, magnification 20 000 $\times$ ; (c) Aldrich AC, magnification 30 000 $\times$ ; (d) Merck AC, magnification 20 000 $\times$ .



developed porosity was clearly visible at a magnification of 20 000 $\times$  and thereby confirmed the high  $S_{\text{BET}}$  value obtained for this sample.

The scanning electron micrographs of the commercial-grade materials revealed a significantly greater uniform porosity for the Merck sample and a somewhat lesser one for the Aldrich specimen.

## Phenol and 4-chlorophenol adsorption

### *Effect of pH on the adsorption capacity*

Figures 6 and 7 present the effect of the initial pH on the adsorption of phenol and 4-chlorophenol onto the activated carbons studied. The adsorption of phenols from aqueous solution depends on the acid–base character of the carbon surface as well as the acidic character of the solute molecules. It should be noted that both phenol and 4-chlorophenol are weak acids with  $\text{pK}_{\text{a}}$  values of 9.89 and 9.40, respectively (Alvarez *et al.* 2005). The lower acidic character of 4-chlorophenol is associated with an electron-withdrawing effect arising from the substitution of chlorine in the aromatic ring. Interactions between the carbon surface and phenols arise from dispersion effects, i.e. aromatic ring–carbon  $\pi$ -electrons, electron donor–acceptor interaction and electrostatic attraction–repulsion in the presence of ions (Coughlin and Ezra 1968).

For the three adsorbents studied, the surface groups are positively charged or neutral at low pH values, with interaction between the carbon surfaces and phenol arising primarily from dispersion effects and electron donor–acceptor interactions. However, enhanced adsorption was observed for 4-chlorophenol due to additional interactions between the electronegative chlorine substituents and the protonated carbon surfaces (Junga *et al.* 2001). This effect is particularly marked in the olive stone-based carbon due to the more acidic surface obtained arising from the phosphoric acid

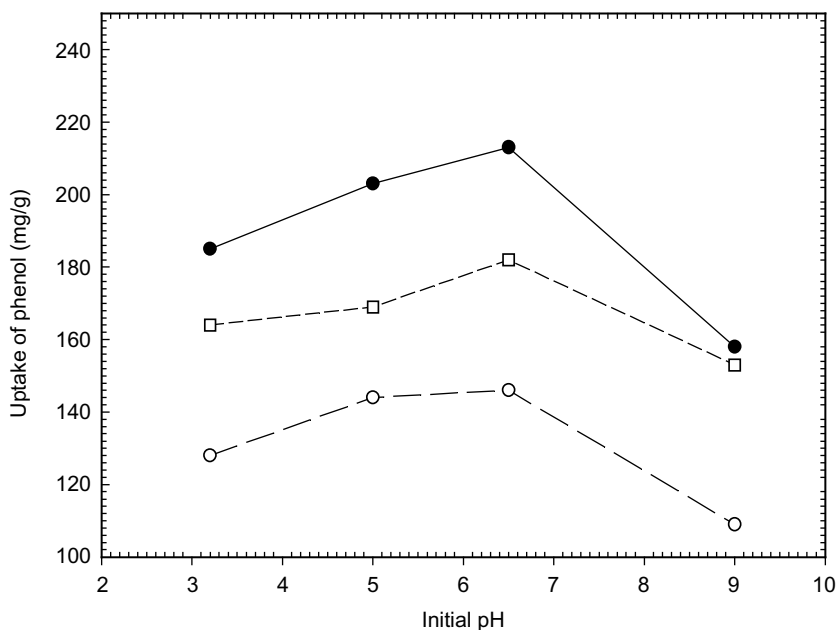


**Figure 6.** Influence of initial solution pH on the adsorption of phenol at an initial concentration,  $C_0$ , of 1000 mg/l. The data points correspond to the following activated carbon (AC) samples: ●, olive stone AC; ○, Merck AC; □, Aldrich AC.

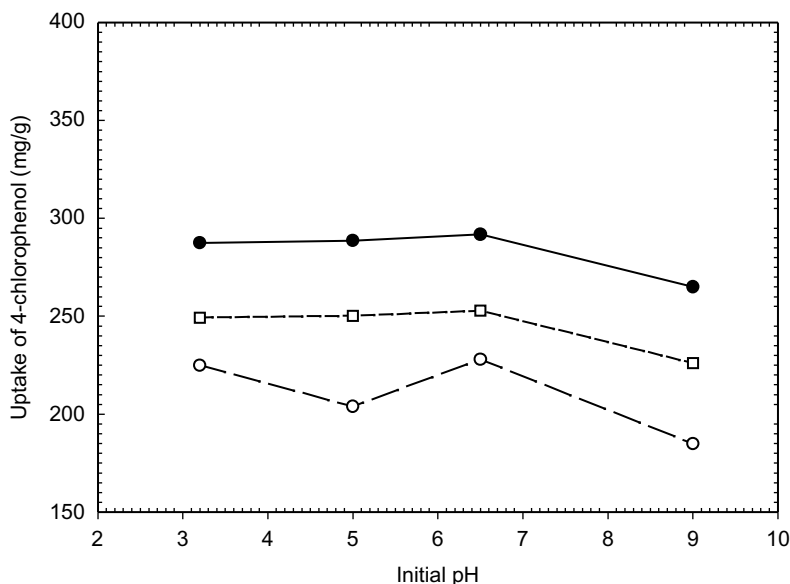


**Figure 7.** Influence of initial solution pH on the adsorption of 4-chlorophenol at an initial concentration,  $C_0$ , of 1600 mg/l. The data points correspond to the following activated carbon (AC) samples: ●, olive stone AC; ○, Merck AC; □, Aldrich AC.

activation method used. For the commercial-grade carbons, a high 4-chlorophenol uptake was obtained at pH values in the range 7–9 in accordance with its  $pK_a$  value, but all three interaction mechanisms might be involved. The adsorption capacity decreased for both solutes at higher pH values due to repulsion between the phenolate ions formed and like charges on the surface.

#### Adsorption isotherms

The adsorption capacities for phenol and 4-chlorophenol were studied at the appropriate pH values for both pollutants. Figures 8 and 9 show the adsorption isotherms of phenol and 4-chlorophenol onto the activated carbons studied, respectively. The Langmuir model was fitted to all the data with the constants being obtained by non-linear regression analysis. This model described the adsorption data for phenol well, as reflected by the equations obtained and regression coefficients ranging from 0.96 to 0.98 (see Table 3). Likewise, the adsorption data for 4-chlorophenol were also well-described by this model with the equations obtained and regression coefficients being listed in Table 4.

The maximum adsorption capacities of the two adsorbents for the two adsorbents were computed from the Langmuir constants and were as recorded in Tables 3 and 4. The olive stone-based activated carbon yielded the highest uptake for phenol as well as 4-chlorophenol with values of 189 mg/g and 436 mg/g, respectively, whereas the Merck carbon attained values of 145 mg/g and 244 mg/g while the Aldrich carbon gave values of 176 mg/g and 316 mg/g, respectively. Lower values are recorded in the literature for the adsorption of phenol and 4-chlorophenol onto commercial-grade activated carbons, viz. 89 mg/g for phenol (Tancredi *et al.* 2004) and 387 mg/g for 4-chlorophenol (Aksou and Yener 2001). Hence, activated carbons prepared from olive stones exhibited a high uptake potential towards the two pollutants.

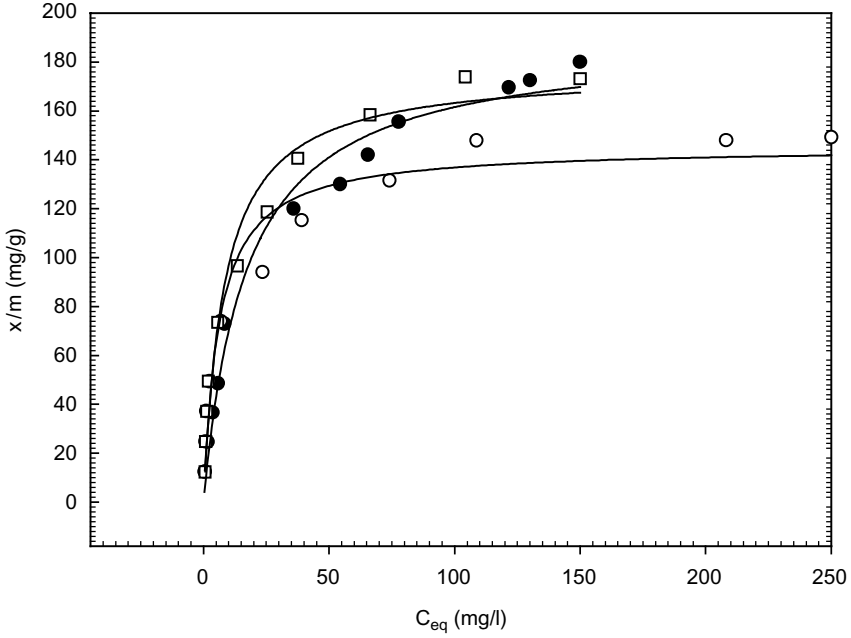


**Figure 8.** Adsorption isotherms for phenol onto the activated carbons studied. Data points correspond to the following activated carbon (AC) samples: ●, olive stone AC; ○, Merck AC; □, Aldrich AC. The full lines in the diagram correspond to the application of the Langmuir isotherm to the corresponding experimental data.

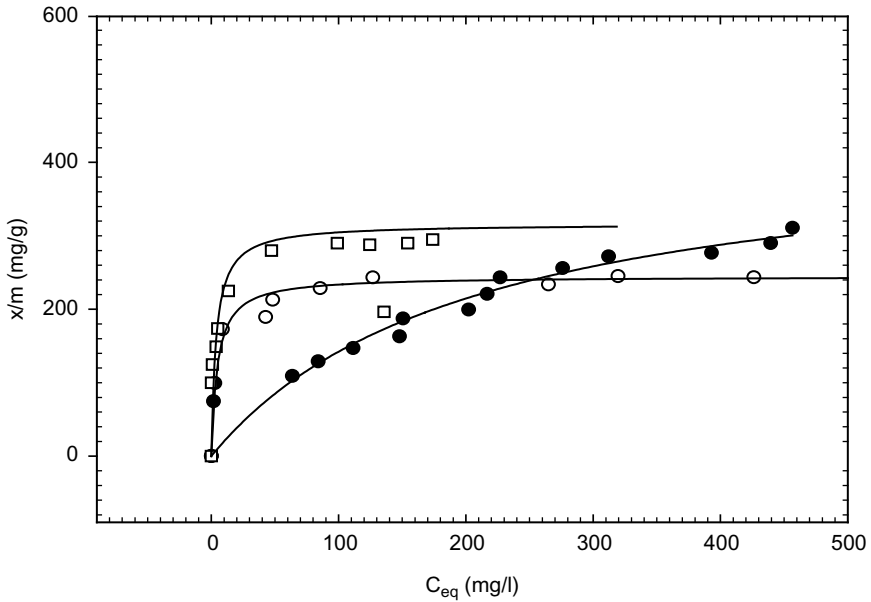


**Figure 9.** Adsorption isotherms for 4-chlorophenol onto the activated carbons studied. Data points correspond to the following activated carbon (AC) samples: ●, olive stone AC; ○, Merck AC; □, Aldrich AC. The full lines in the diagram correspond to the application of the Langmuir isotherm to the corresponding experimental data.

**TABLE 3.** Langmuir Equations and Constants for Phenol Adsorption by Olive-stone, Aldrich and Merck Activated Carbons (AC)

Adsorbent	Langmuir equation	R <sup>2</sup>	K (l/mg)	b (mg/g)
Olive-stone AC	$x/m = 11.1039C_{eq}/(1 + 0.0587C_{eq})$	0.98	0.0587	189
Merck AC	$x/m = 23.611C_{eq}/(1 + 0.1625C_{eq})$	0.96	0.1625	145
Aldrich AC	$x/m = 21.734C_{eq}/(1 + 0.1213C_{eq})$	0.97	0.1213	179

**TABLE 4.** Langmuir Equations and Constants for 4-Chlorophenol Adsorption by Olive-stone, Merck and Aldrich Activated Carbons (AC)

Adsorbent	Langmuir equation	R <sup>2</sup>	K (l/mg)	b (mg/g)
Olive-stone AC	$x/m = 2.108C_{eq}/(1 + 0.0048C_{eq})$	0.96	0.0048	436
Merck AC	$x/m = 51.016C_{eq}/(1 + 0.2084C_{eq})$	0.99	0.2084	244
Aldrich AC	$x/m = 83.91C_{eq}/(1 + 0.2654C_{eq})$	0.86	0.2654	316

## CONCLUSIONS

This study has dealt with the production of activated carbons from olive stones by chemical activation using 50% phosphoric acid as the activating agent. The results indicate that activation temperature and time led to increased surface area due to pore creation and enlargement. Nitrogen gas and Methylene Blue adsorption as well as iodine number indicated both a high surface area and a mixed microporous/mesoporous structure for the activated carbons thus prepared. The high adsorption capacities exhibited towards phenol and 4-chlorophenol relative to commercial-grade activated carbons may be accounted for by the high surface area, larger pore size of the mesoporous adsorbent and also by the existence of additional sites for adsorption provided by the carbon–oxygen functional groups present on the carbon surface.

In conclusion, olive stones provide a good precursor for the production of viable activated carbons with very interesting properties. These can be utilized successfully in pollution remediation of aqueous environments.

## REFERENCES

- Aksou, Z. and Yener, J. (2001) *Waste Manage.* **21**, 685.
- Alvarez, P.M., Garcia-Araya, J.F., Beltran, F.J., Masa, F.J. and Medina, F. (2005) *J. Colloid Interface Sci.* **283**, 503.
- ASTM (1999) "Standard Test Method for Determination of Iodine Number of Activated Carbon", ASTM Annual Book, Section 15, Vol. 4, D4607-94.
- Aygün, A., Yenisoay-Karakaş, S. and Duman, I. (2003) *Microporous Mesoporous Mater.* **66**, 189.
- Bansal, R.C., Dhama, T.L. and Parkash, S. (1977) *Carbon* **15**, 157.
- Benderdouche, N., Bestani, B., Benstaali, B. and Derriche, Z. (2003) *Adsorp. Sci. Technol.* **21**, 8.
- Boehm, H.P. (1966) *Adv. Catal.* **16**, 179.

- Boehm, H.P. (1994) *Carbon* **32**, 759.
- Coughlin, R.W. and Ezra, F.S. (1968) *Environ. Sci. Technol.* **2**, 291.
- Dubinini, M.M. (1985) *Carbon* **23**, 473.
- Dubinini, M.M. (1989) *Carbon* **27**, 457.
- El-Sheikh, A.H., Newman, A.P., Al-Daffaee, H.K., Phull, S. and Cresswell, N. (2004) *J. Anal. Appl. Pyrol.* **71**, 1.
- Galiatsatou, P., Metaxas, M. and Kasseloui-Rigopoulou, V. (2001) *Mikrochim. Acta* **136**, 147.
- Gardea-Torresdey, J.L., Gonzalez, J.H., Tiemann, K.J., Rodriguez, O. and Gamez, G. (1998) *J. Hazard. Mater.* **57**, 29.
- Gimeno, O., Carbajo, M., Beltran, F. and Rivas, F.J. (2005) *J. Hazard. Mater. B1* **19**, 99.
- Gómez-Serrano, V., Cuerda-Correa, E.M., Fernández-González, M.F., Alexandre-Franco, A. and Macias-Garcia, A. (2005) *Mater. Lett.* **59**, 846.
- Gonzales-Serrano, E., Cordero, T., Rodríguez-Mirasol, J. and Rodriguez, J.J. (1997) *Ind. Eng Chem., Res.* **36**, 4832.
- Goyal, M., Rattan, V.K. and Bansal, R.C. (2001) *Colloids Surf. A* **229**, 190.
- Goyal, M., Singh, S. and Bansal, R.C. (2004) *Carbon Sci.* **5**, 170.
- Hamadi, N.K., Chen, X.D., Farid, M.M. and Lu, Max G.Q. (2001) *Chem. Eng. J. (Lausanne)* **84**, 95.
- Junga, M.-W., Ahna, K.-H., Leea, Y., Kimb, K.-P., Rheec, J.-S., Park, J.T. and Paeng, K.-J. (2001) *Microchem. J.* **70**, 123.
- Leon y Leon, C.A. and Radovic, L.R. (1992) *Chem. Phys. Carbon* **24**, 213.
- Lucier, M.G., Shull, J.C. and Miller, D.J. (1994) *Carbon* **32**, 8.
- Martinez, M.L., Moiraghi, L., Agnese, M. and Guzman, C. (2003) *J. Argent. Chem. Soc.* **91**, 103.
- Mattson, J.S. and Mark, Jr., H.B. (1971) *Activated Carbon Surface Chemistry and Adsorption from Solution*, Marcel Dekker, New York.
- Milner, C.R. and Goulder, R. (1986) *Bull. Environ. Contam. Toxic.* **37**, 714.
- Molina-Sabio, M. and Rodríguez-Reinoso, F. (2004) *Colloids Surf. A* **241**, 15.
- Ng, C., Marshall, W.E., Rao, R.M., Bansode, R.R. and Losso, J.N. (2003) *Indian Crops Prod.* **17**, 209.
- Noszko, L., Bota, A., Simay, A. and Nagy, L.G. (1984) *Period. Polytech.* **28**, 293.
- Plaza de los Reyes, J., Orellana, F. and Urizar, S. (1997) *Bol. Soc. Chil. Quim.* **42**, 493.
- Stavropoulos, G.G. and Zabaniotou, A.A. (2005) *Microporous Mesoporous Mater.* **82**, 79.
- Tancredi, N., Medero, N., Moller, F., Piriz, J., Carina, P. and Cordero, T. (2004) *J. Colloid Interface Sci.* **279**, 357.
- Yan, G. and Viraraghavan, T. (2000) *Water SA* **26**, 119.

